Progress In Electromagnetics Research B, Vol. 28, 273–287, 2011

MUTUAL INDUCTANCE FOR AN EXPLICITLY FINITE NUMBER OF TURNS

J. T. Conway

University of Agder
9 Lilletuns Vei, Grimstad 4879, Norway

Abstract—Non coaxial mutual inductance calculations, based on a Bessel function formulation, are presented for coils modelled by an explicitly finite number of circular turns. The mutual inductance of two such turns can be expressed as an integral of a product of three Bessel functions and an exponential factor, and it is shown that the exponential factors can be analytically summed as a simple geometric progression, or other related sums. This allows the mutual inductance of two thin solenoids to be expressed as an integral of a single analytical expression. Sample numerical results are given for some representative cases and the approach to the limit where the turns are considered to be smeared out over the solenoid windings is explored.

1. INTRODUCTION

The formula encountered most frequently for calculating the mutual inductance M_{21} of two coaxial circular loops of radii R_1 and R_2 which lie in the parallel planes $z = z_1$ and $z = z_2$ is the elliptic integral formula:

$$M_{21} = \mu_0 \frac{\sqrt{R_1 R_2}}{k} \left[\left(2 - k^2\right) \mathbf{K}\left(k\right) - 2\mathbf{E}\left(k\right) \right] \tag{1}$$

where

$$k = \sqrt{\frac{4R_2R_1}{\left(R_2 + R_1\right)^2 + \left(z_2 - z_1\right)^2}}. \tag{2}$$

In Equations (1) and (2), μ_0 is the permeability of free space and z is the axial coordinate of a cylindrical coordinate system (r, ϕ, z). These formulas are frequently used to calculate the mutual inductance of two

Received 1 November 2010, Accepted 28 February 2011, Scheduled 2 March 2011
Corresponding author: John Thomas Conway (John.Conway@uia.no).

complete coils, each with a finite number of turns, by summing over all the loop pairings between the coils. A primary disadvantage of Equations (1) and (2) is that they are restricted to the coaxial case.

It has long been known that the mutual inductance can also be expressed as an equivalent integral involving Bessel functions:

$$M_{21} = \mu_0 \pi R_1 R_2 \int_0^\infty J_1(sR_1)\, J_1(sR_2) \exp(-s\,|z_2 - z_1|)\, ds. \qquad (3)$$

Havelock [1] used Equation (3) to obtain series solutions for coaxial coils but historically Equation (3) has been mostly ignored. The problem has been that the integral in Equation (3) is highly oscillatory and it is only fairly recently that computer packages such as Mathematica [2] have appeared which can evaluate (3) to high accuracy. Even today, evaluation of (3) is much slower than evaluation of (1) and (2). Numerical experimentation with Mathematica [2] indicated that numerical evaluation of Equation (3) requires a factor of approximately 10^3 more cpu time to evaluate to high accuracy (30 significant figures) than Equations (1) and (2). This estimate is somewhat fluid and is changing with algorithm development.

It is to be noted that the geometric parameters in (3) are separated out as individual factors, and this allows (3) to be analytically integrated radially and axially to give formulas for the mutual inductance of complete coils, in the approximation where the finite number of turns for each coil are considered to be smeared out over the windings of the coils. A typical pair of non coaxial coils is shown schematically in Figure 2. The coils are considered to consist of a discrete number of turns, with in general different turn spacings in the radial and axial directions. The coils have inner radii $R_{in}^{(1)}$ and $R_{in}^{(2)}$, outer radii $R_{out}^{(1)}$ and $R_{out}^{(2)}$, and axial lengths L_1 and L_2. The individual turns lie in the planes $z = z_i$ and $z = z_j$ and the coil axes are separated by a perpendicular distance p. Thick coils can be considered to consist of either of axial stacks of annular ring coils or radial stacks of thin solenoids.

Equation (3) has been extended [3] to the non coaxial case shown in Figure 1 using Neumann's addition theorem for Bessel functions [4]:

$$J_0\left(s\sqrt{R_2^2 + p^2 - 2pR_2\cos\phi}\right)$$
$$= J_0(sp)\, J_0(sR_2) + 2\sum_{n=1}^{\infty} J_n(sp)\, J_n(sR_2)\cos(n\phi) \qquad (4)$$

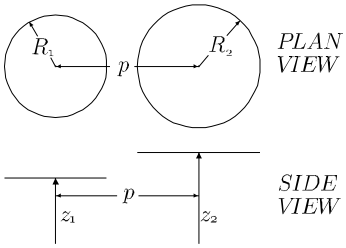

Figure 1. Circular loops of radii R_1 and R_2 lying in parallel planes $z = z_1$ and $z = z_2$ and separated by a perpendicular distance p.

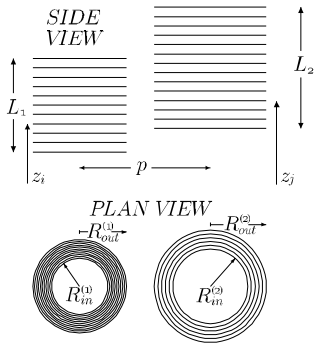

Figure 2. Two thick solenoids constructed of discrete turns.

to give the simple generalization:

$$M_{21} = \mu_0 \pi R_1 R_2 \int_0^\infty J_0(sp)\, J_1(sR_1)\, J_1(sR_2) \exp(-s\,|z_2 - z_1|)\, ds. \quad (5)$$

Equation (5) can be obtained more directly than in [3] using Graf's generalization of Neumann's theorem [4, 5]. For two coplanar loops with $z_2 = z_1$, Equation (5) reduces to

$$M_{21} = \mu_0 \pi R_1 R_2 \int_0^\infty J_0(sp)\, J_1(sR_1)\, J_1(sR_2)\, ds \quad (6)$$

and this integral can be evaluated in closed form in terms of Legendre functions using the results given by Gervois and Navelet [6]. Using the addition theorem (4), Equation (5) can be expressed in the form

$$M_{21} = \mu_0 R_1 R_2 \int_0^\infty \int_0^\pi \cos(\phi) J_0(sp) J_0(s\chi(\phi)) \exp(-s|z_2 - z_1|) d\phi ds \quad (7)$$

where

$$\chi(\phi) = \sqrt{R_1^2 + R_2^2 - 2R_1 R_2 \cos\phi} \quad (8)$$

and the integral with respect to s in Equation (7) can be evaluated in terms of a Legendre function of the second kind [4, 7] to give

$$M_{21} = \frac{\mu_0 R_1 R_2}{\pi} \int_0^\pi \frac{\cos(\phi)}{\sqrt{p\chi(\phi)}} Q_{-1/2}\left(\frac{p^2 + \chi^2(\phi) + (z_2 - z_1)^2}{2p\chi(\phi)}\right) d\phi. \quad (9)$$

The Legendre function in (9) can be expressed in terms of a complete elliptic integral of the first kind [8] to give the alternative expression

$$M_{21} = \frac{2\mu_0 R_1 R_2}{\pi} \int_0^{\pi} \frac{\cos(\phi)\, \mathbf{K}\left(\hat{k}(\phi)\right)}{\sqrt{(p+\chi(\phi))^2 + (z_2 - z_1)^2}} d\phi \tag{10}$$

where

$$\hat{k}(\phi) = \sqrt{\frac{4p\chi(\phi)}{(p+\chi(\phi))^2 + (z_2 - z_1)^2}}. \tag{11}$$

The integrals (9) and (10) are more numerically robust alternatives to Equation (5).

When calculating the mutual inductance of two thick coils by smearing the turns over the coil windings [9], integration of Equation (5) gives rise to only one integral of Bessel and Struve functions. For the discrete case, integration is replaced with summation over the various combinations of pairs of turns. It is undesirable to have an integral such as (5) for each turn pair combination, and fortunately this can be avoided by summing the axial factors resulting from Equation (5) using the elementary formula

$$\sum_{n=0}^{N} x^n = \frac{1 - x^{N+1}}{1 - x} \tag{12}$$

and similar summations derived from this one. This allows the mutual inductance of two thin cylindrical solenoids to be evaluated as a single integral not significantly more complex than Equation (5). The mutual inductance of two thick coils can then obtained by summing over the various combinations of thin solenoids. With current knowledge, it does not seem to be possible to sum analytically in the radial direction in the same manner as in the axial direction.

The work presented here is essentially the non coaxial Bessel function equivalent of the filamentary method based on elliptic integrals. The filamentary method has been applied successfully to non coaxial cases by Akyel, Babic and Mahmoudi [10].

The special functions used in the analysis presented here are given in Table 1.

Table 1. Special functions used.

Symbol	Special Function
$E(\beta, k)$	Elliptic integral of the second kind
$E(k)$	Complete elliptic integral of the second kind
$F(\beta, k)$	Elliptic integral of the first kind
$H(x)$	Heaviside step function
$J_\nu(x)$	Bessel function of the first kind
$K(k)$	Complete elliptic integral of the first kind
$Q_\mu(\omega)$	Legendre function of the second kind
$\mathrm{sgn}(x)$	-1, 0, or $+1$ for x negative, zero, or positive
$\delta(x)$	Dirac delta function
$\Lambda_0(\beta, k)$	Heuman's Lambda function

2. FORMULATION

The vector potential of a circuit C_1 carrying a current of one amp is given by

$$\mathbf{A}_1(\mathbf{r}) = \frac{\mu_0}{4\pi} \oint_{C_1} \frac{d\mathbf{r}_1}{|\mathbf{r} - \mathbf{r}_1|}. \tag{13}$$

If C_1 is a circular turn of radius R_1, located in the plane $z = z_1$ of cylindrical coordinates (r, ϕ, z) and centred on the cylindrical axis, then Equation (13) becomes

$$\mathbf{A}_1(\mathbf{r}) = \frac{\mu_0 R_1}{2\pi} \int_0^\pi \frac{\cos\phi}{\sqrt{R^2 + r^2 + (z - z_1)^2 - 2R_1 r\cos\phi}}. \tag{14}$$

Equation (14) can be expressed in terms of complete elliptic integrals as

$$\mathbf{A}_1(\mathbf{r}) = \frac{\mu_0}{2\pi}\sqrt{\frac{R_1}{r}}\left(\frac{\left(2 - \bar{k}^2\right)\mathbf{K}\left(\bar{k}\right) - 2\mathbf{E}\left(\bar{k}\right)}{\bar{k}}\right) \tag{15}$$

where

$$\bar{k} = \sqrt{\frac{4R_1 r}{(R_1 + r)^2 + z^2}} \tag{16}$$

or alternatively as an integral involving a product of Bessel functions [3]:

$$\mathbf{A}_1(\mathbf{r}) = \frac{\mu_0 R_1}{2} \int_0^\infty J_1(sR_1)\, J_1(sr) \exp\left(-s\,|z - z_1|\right) ds. \tag{17}$$

The mutual inductance M_{21} of the circuit C_1 with another circuit C_2 is given by

$$M_{21} = \oint_{C_2} \mathbf{A}_1(\mathbf{r}_2) \cdot d\mathbf{r}_2 \tag{18}$$

and if C_2 is a coaxial circular loop of radius R_2, then substitution of (15)–(16) and Equation (17) into Equation (18) gives Equations (1) and (3) respectively.

For the non coaxial case shown in Figure 3, substitution of Equation (17) into Equation (18) and exploiting the symmetry properties of the integrand gives

$$\begin{aligned} M_{21} \;=\; & \mu_0 R_1 R_2 \times \int_0^{\infty}\int_0^{\pi} J_1(sR_1)\exp(-s|z_2-z_1|) \\ & \cos\psi J_1\left(s\sqrt{p^2+R_1^2+2pR_2\cos\phi'}\right)d\phi' ds \end{aligned} \tag{19}$$

where $r \equiv \sqrt{p^2+R_1^2+2pR_2\cos\phi'}$ and $\psi \equiv \mathbf{e}_\phi \cdot \mathbf{e}_{\phi'}$ is the angle between the vector $\mathbf{A}_1(\mathbf{r}_2)$ and the line element $d\mathbf{r}_2$. The angles ϕ, ϕ' and $\psi \equiv \phi' - \phi$ are shown in Figure 3. The factor $\cos\psi J_1(s\sqrt{p^2+R_2^2-2pR_2\cos\phi'})$ can be expanded as a Fourier series in ϕ' using Graf's addition theorem [4, 5] to give

$$\begin{aligned} & \cos(\psi)\, J_1\left(s\sqrt{p^2+R_2^2-2pR_2\cos\phi'}\right) \\ = \;& J_1(sR_2)\, J_0(sp) + 2\sum_{m=1}^{\infty} J_{m+1}(sR_2)\, J_m(sp)\cos\left(m\phi'\right), \end{aligned} \tag{20}$$

valid for all ψ. When Equation (20) is substituted into Equation (19), only the first term survives to give Equation (3). The non coaxial

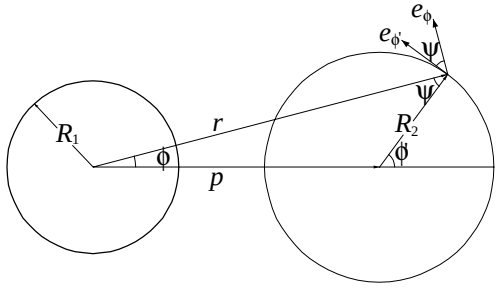

Figure 3. Geometry for Graf's addition theorem.

Equation (5) is no more time consuming to evaluate numerically than the coaxial Equation (3). However, no non coaxial elliptic integral equivalent of Equations (1) and (2) has yet been found, and filamentary approaches using elliptic integrals are forced to treat the non coaxial case by numerical integration of Equation (15) around the secondary coil. Depending on the accuracy demanded, this reduces the advantage of an elliptic integral approach, for a single pair of non coaxial loops, to somewhere between 10^2 and 10. Romberg integration of Equation (15) around the circumference of the the secondary loop is employed in [10].

2.1. Application to Finite Solenoids

The geometric parameters occur as separate factors in Equation (3), which allows axial and radial integrations to give the mutual inductance of finite solenoids where the discrete turns of the two solenoids are considered to be smeared out over the cross sections of the coils. Integration of the Bessel functions presents no difficulties, but a complication arises from the modulus sign in the exponential, since either

$$\exp\left(-s\left|z_2 - z_1\right|\right) = \exp\left(-sz_1\right)\exp\left(sz_2\right) \text{ for } [z_1 > z_2]$$

or

$$\exp\left(-s\left|z_2 - z_1\right|\right) = \exp\left(sz_1\right)\exp\left(-sz_2\right) \text{ for } [z_2 > z_1].$$

Hence inductance cases must be treated differently depending on whether there is axial overlap or not. When the inductance is calculated by smearing the turns over the solenoid windings, the three cases shown schematically in Figure 4 are sufficient. However, when the discrete nature of the turns is considered, additional sub-cases must be analyzed.

3. NO OVERLAP CASE

The generic case of no overlap is the simplest to analyze and is shown schematically in Figure 5. No particular relationship between the turn pitches $L_1/(N_1 - 1)$ and $L_2/(N_2 - 1)$ need be assumed in this case. The mutual inductance is given by

$$M_{21} = \mu_0 \pi R_1 R_2 \times \int_0^\infty J_0(sp) J_1(sR_1) J_1(sR_2) \left(\sum_{n=0}^{N_1-1} \sum_{m=0}^{N_2-1} \exp(-s|z_n - z_m|) \right) ds \quad (21)$$

and for this case each of the exponential factors satisfies:

$$\exp\left(-s\left|z_n - z_m\right|\right) = \exp\left(-sz_m\right)\exp\left(sz_n\right) \quad (22)$$

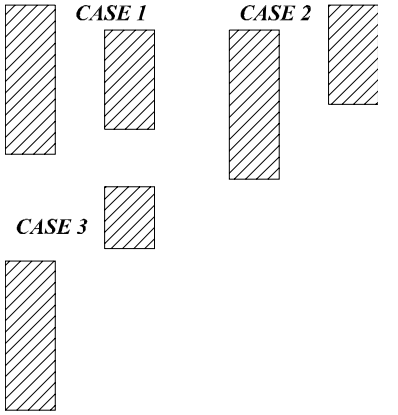

Figure 4. Distinct solenoid overlap cases.

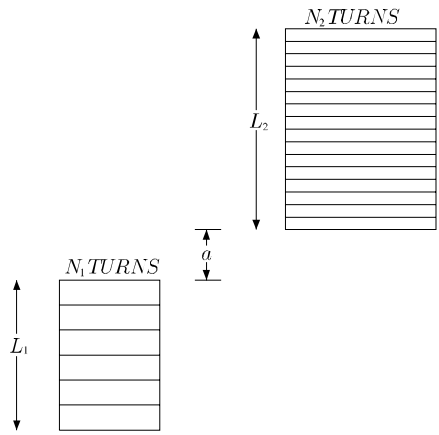

Figure 5. Non coaxial solenoids with no axial overlap.

where the index m is assumed to run over the turns of the coil with the largest axial coordinates. It is convenient to measure the axial coordinate from the top of the stack of turns of Coil 1, as shown in Figure 5, which gives

$$z_n = -\frac{nL_1}{N_1 - 1} \tag{23}$$

$$z_m = a + \frac{mL_2}{N_2 - 1} \tag{24}$$

and the double summation in Equation (21) becomes

$$\sum_{n=0}^{N_1-1} \sum_{m=0}^{N_2-1} \exp\left(-s\left|z_n - z_m\right|\right)$$

$$= \exp\left(-sa\right) \sum_{n=0}^{N_1-1} \sum_{m=0}^{N_2-1} \exp\left(-s\frac{nL_1}{N_1 - 1}\right) \exp\left(-s\frac{mL_2}{N_2 - 1}\right). \tag{25}$$

This summation can be evaluated using Equation (12), which gives the inductance as

$$M_{21} = \mu_0 \pi R_1 R_2 \int_0^\infty J_0\left(sp\right) J_1\left(sR_1\right) J_1\left(sR_2\right)$$

$$\times \exp\left(-sa\right) \frac{1 - \exp\left(-s\frac{N_1 L_1}{N_1 - 1}\right)}{1 - \exp\left(-s\frac{L_1}{N_1 - 1}\right)} \frac{1 - \exp\left(-s\frac{N_2 L_2}{N_1 - 1}\right)}{1 - \exp\left(-s\frac{L_2}{N_2 - 1}\right)} ds. \tag{26}$$

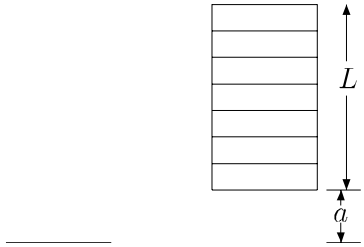

Figure 6. A coil with N turns and a non overlapping single turn.

If one of the coils consists of a single turn and the second coil has N turns and length L, as shown in Figure 6, then Equation (26) reduces to

$$M_{21} = \mu_0 \pi R_1 R_2 \times \int_0^\infty J_0(sp) J_1(sR_1) J_1(sR_2) \exp(-sa) \frac{1-\exp\left(-s\frac{NL}{N-1}\right)}{1-\exp\left(-s\frac{L}{N-1}\right)} ds. \quad (27)$$

Evaluation of Equation (26) has essentially the same computational cost regardless of the number of turns in the coils and is the principal result presented here. Equation (26) can be compared with the corresponding formula given in [3] for the case where the turns are considered to be smeared out over the coil windings:

$$M_{21} = \frac{\mu_0 \pi N_1 N_2 R_1 R_2}{(d_1 - c_1)(b_1 - a_1)} \int_0^\infty J_0(sp) J_1(sR_1) J_1(sR_2) f(s) ds \quad (28)$$

where

$$f(s) = +\frac{\exp(-s(c_1 - b_1)) - \exp(-s(d_1 - b_1))}{s^2} + \frac{\exp(-s(d_1 - a_1)) - \exp(-s(c_1 - a_1))}{s^2} \quad (29)$$

and in this case

$$a_1 = 0 \quad (30)$$

$$b_1 = L_1 \quad (31)$$

$$c_1 = L_1 + a \quad (32)$$

$$d_1 = L_1 + L_2 + a. \quad (33)$$

Table 2 gives values of $M_{21}/(N_1 N_2)$ as N_1 and N_2 are increased, calculated with Equation (26). For comparison, the ratio of M_{21}

Table 2. Mutual inductance of two coils with no axial overlap. The values of the geometric parameters in metres are: $R_1 = 1$, $R_2 = 2$, $p = 0.5$, $L_1 = 2$, $L_2 = 4$ and $a = 1$.

N_1	N_2	$M_{21}/(N_1N_2)\,\mu F/\text{turn}^2$	Discrete/Continuous
2	4	0.1681055355249557	1.428582568227190
4	8	0.1355886265972299	1.152249673407768
8	16	0.1254934023899186	1.066459153304585
10	20	0.1237738380992955	1.051846073712298
100	200	0.1182327677621735	1.004757341814126
200	400	0.1179515824161245	1.002367792400705
400	800	0.1178119519219559	1.001181194414272
800	1600	0.1177423753806299	1.000589923973442
1000	2000	0.1177284791021068	1.000471831602483
10^4	2×10^4	0.1176785049115029	1.000047144471658
10^5	2×10^5	0.1176735119995567	1.000004714060614
10^6	2×10^6	0.1176730127533939	1.000000471402196
10^9	2×10^9	0.1176729573375747	1.000000000471402
10^{12}	2×10^{12}	0.1176729572821589	1.000000000000471
10^{15}	2×10^{15}	0.1176729572821035	1.000000000000000

calculated with Equation (26) to that given by Equations (28)–(33) is also shown. It can be seen from this table that the discrete inductance and the inductance calculated by smearing out the turns over the windings tend to each other only logarithmically as the number of turns is increased. For coils with only a moderate number of turns, the difference is significant.

4. SOLENOIDS WITH AXIAL OVERLAP

Figure 7 shows the general discrete case with axial overlap. It is more complicated than the continuous case, which reduces to a few explicit formulas [3]. An exception is when one coil consists of a single turn. Then the case can be split into the sum of the two non-overlapping cases shown in Figure 8. The general overlap case shown in Figure 7 can be regarded as a sum of cases such as that shown in Figure 8. This is better than simply summing over all combinations of turns, but ideally we want to do better than this, with full analytical summation if possible. However, if one of the solenoids has relatively few turns, this approach has the advantage of simplicity.

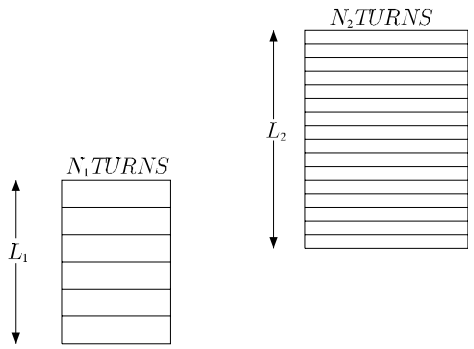

Figure 7. Generic discrete overlap case. If the coils have different radii the smaller coil may lie partially within the larger.

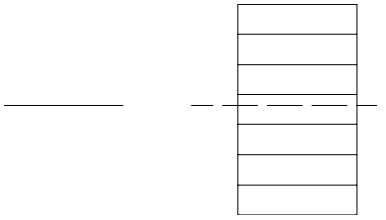

Figure 8. A coil with N turns and an overlapping single turn.

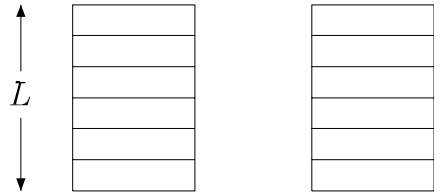

Figure 9. Two fully overlapping coils, each of length L and with N turns each. The radii of the coils need not be equal and the smaller coil may lie within the larger.

4.1. Two Fully Overlapping Coils with the Same Length and Turn Pitch

A starting point for a more general overlap solution is the pair of fully overlapping coils shown in Figure 9. The axial exponential factors in this case can be expressed as:

$$\sum_{n=0}^{N-1}\sum_{m=0}^{N-1}\exp(-s|z_n-z_m|) = N + 2\sum_{n=1}^{N-1}(N-n)\left(\exp\left(-\frac{sL}{N-1}\right)\right)^n \quad (34)$$

and this can be evaluated using the elementary summation:

$$N + 2\sum_{n=1}^{N-1}(N-n)\,x^n = N + 2x\left(\frac{x^N-1}{(1-x)^2} + \frac{N}{1-x}\right). \quad (35)$$

This gives the multiplicative factor arising from the sum of the axial terms as:

$$f_1(s) = N + 2\exp\left(-\frac{sL}{N-1}\right)\left(\frac{\exp\left(-\frac{sNL}{N-1}\right)-1}{\left(1-\exp\left(-\frac{sL}{N-1}\right)\right)^2}+\frac{N}{1-\exp\left(-\frac{sL}{N-1}\right)}\right). \quad (36)$$

The corresponding factor for this case in the approximation where the turns are considered to be delocalized over the coil windings is [3]

$$f_2(s) = 2\left(\frac{L}{s}+\frac{\exp(-sL)}{s^2}-\frac{1}{s^2}\right). \quad (37)$$

Equations (35) and (37) both contain terms without exponential decays, which could be evaluated analytically [3]. Sample numerical results for this case, calculated using Equations (36) and (37), are given in Table 3.

Table 3. Mutual inductance for two fully overlapping coils with the same length and turn pitch. The values of the geometric parameters in metres are: $R_1 = 1$, $R_2 = 2$, $p = 0.5$ and $L = 2$. The smaller coil is completely within the larger.

N	$M_{21}/(N^2)\,\mu F/\text{turn}^2$	Discrete/Continuous
2	0.7491855021351923	0.8464865122913206
4	0.7967893017949642	0.9002728899387401
8	0.8424680854228049	0.9518842387016841
10	0.8512804345168687	0.9618410980221967
100	0.8817748761391568	0.9962960273548573
200	0.8834165496739562	0.9981509144299979
400	0.8842354572439289	0.9990761782142269
800	0.8846444319734841	0.9995382688332389
1000	0.8847261887136125	0.9996306437892550
10^4	0.8850204077266067	0.9999630747098340
10^5	0.8850498205758672	0.9999963075742129
10^6	0.8850527617703432	0.9999996307584535
10^9	0.8850530882419161	0.9999999996307586
10^{12}	0.8850530885683876	0.9999999999996308
10^{15}	0.8850530885687141	1.000000000000000

5. TWO COILS OF THE SAME LENGTH AND TURN PITCH DISPLACED BY A DISTANCE LESS THAN THE PITCH

This case is shown schematically in Figure 10. For this case the exponential factor given in Equation (35) generalizes to give

$$f_3(s) = N\exp(-s\Delta z) + 2\cosh(s\Delta z)\sum_{n=1}^{N-1}(N-n)\left(\exp\left(-\frac{sL}{N-1}\right)\right)^n \quad (38)$$

and on evaluating the summation this becomes

$$f_3(s) = N\exp(-s\Delta z) + 2\cosh(s\Delta z)\exp\left(-\frac{sL}{N-1}\right) \times\left(\frac{\exp\left(-\frac{sNL}{N-1}\right)-1}{\left(1-\exp\left(-\frac{sL}{N-1}\right)\right)}+\frac{N}{1-\exp\left(-\frac{sL}{N-1}\right)}\right). \quad (39)$$

It is to be noted that this expression diverges as $s \to \infty$ for

$$\Delta z > \frac{L}{N-1}.$$

Sample numerical results for this case with $N = 5$ are given in Table 4.

6. GENERAL CASE OF OVERLAPPING COILS

Two partly overlapping coils with the same turn pitch are shown in Figure 11. This case can be solved by splitting it as shown in the

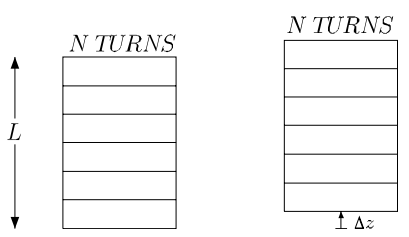

Figure 10. Two coils with the same length and turn pitch, with a relative axial displacement Δz.

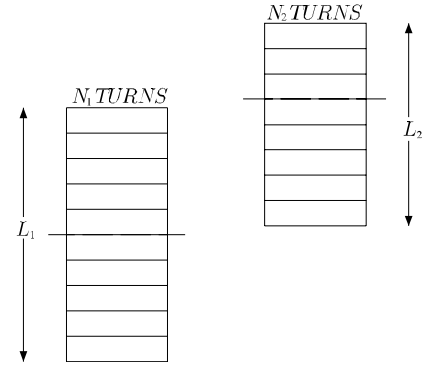

Figure 11. Two overlapping coils with the same turn pitch.

Table 4. Mutual inductance M_{21} for two coils of length L metres and N turns each. The coil radii are $R_1 = 1\,\mathrm{m}$ and $R_2 = 2\,\mathrm{m}$. The coil axes are displaced by a perpendicular distance $p = 0.5\,\mathrm{m}$, so that the smaller coil lies partially inside the larger.

Δz in metres	M_{21} in μF
0	14.038668800139634
0.1	14.007868189152043
0.2	13.923359801741833
0.3	13.804359620604865
0.4	13.672180125973312
0.5	13.542836246459151
0.6	13.423591793706997
0.7	13.312233681646097
0.8	13.198064449358292
0.9	13.065095029475769
1	12.898304947462684

Figure. If the overlapping turns lie in the same axial planes for both coils then (36) is to be used for the overlap, otherwise (39) is to be used.

Pairs of coils with pitches in a fixed ratio can also be solved by superposition of simpler cases, though in the general case these superpositions are complicated. For simplicity's sake it may be preferable to solve the general case by splitting the coil with the fewest turns into single turns and superposing cases such as that shown in Figure 8. If the discreteness of the coils is an issue at all, this must mean that at least one of the pair has a moderate number of turns. This solenoid can then be split into single turns at moderate computational cost.

7. CONCLUSIONS

Two discrete solenoids can be efficiently analyzed with a Bessel function formalism by summing analytically in the axial direction. This allows the approach to the continuous limit to be examined in great detail, as any number of discrete turns has the same computational cost as only a few turns. A number of cases can be analytically summed, but for the completely general case it is more convenient to split one of the solenoids into discrete turns.

The computational advantage of the method presented here

depends on the number of turns and whether or not the case is non coaxial. Assuming (conservatively) that the advantage for the elliptic integral approach over the Bessel function approach is 10^2 for two noncoaxial turns, then the break even point is for two coils with 10 turns each. The calculations presented here for non coaxial coils, where the number of turns is sufficient to approximate the continuous limit to high accuracy, are totally impossible with the elliptic integral approach.

REFERENCES

1. Havelock, T. H., "On certain Bessel integrals and the coefficients of mutual induction of coaxial coils," *Phil. Mag.*, Vol. 15, 332–345, 1908.
2. Wolfram, S., *The Mathematica Book*, 5th edition, Wolfram Media, Champaign, IL, 2003.
3. Conway, J. T., "Inductance calculations for noncoaxial coils using Bessel functions," *IEEE Trans. Mag.*, Vol. 43, No. 3, 1023–1034, 2007.
4. Watson, G. N., *A Treatise on the Theory of Bessel Functions*, 2nd edition, Cambridge, 1944.
5. Graf, J. H., "Ueber die addition und subtraction der argumente bei Bessel'schen functionen nebst einer anwendung," *Math. Ann.*, Vol. 43, 136–144, 1893.
6. Gervois, A. and H. Navelet, "Integrals of three Bessel functions and Legendre functions I and II," *J. Math. Phys.*, Vol. 26, 633–644, 1985.
7. Gradshteyn, I. S. and I. M. Rhyzik, *Table of Integrals, Series and Products*, 7th edition, Academic, New York, 2007.
8. Abramowitz, M. and I. A. Stegun, *Handbook of Mathematical Functions, with Formulas, Graphs and Mathematical Tables*, Dover, New York, 1972.
9. Conway, J. T., "Inductance calculations for circular coils of rectangular cross section and parallel axes using Bessel and Struve functions," *IEEE Trans. Mag.*, Vol. 46, No. 1, 75–81, 2010.
10. Akyel, C., S. I. Babic, and M. M. Mahmoudi, "Mutual inductance calculations for non-coaxial circular air coils with parallel axes," *Progress In Electromagnetics Research*, Vol. 91, 287–301, 2009.